$CuBrSe_2$: a Metastable Compound in the System CuBr/Se

Arno Pfitzner* , **Tom Nilges, and Hans-Jörg Deiseroth**

Siegen, Anorganische Chemie der Universität-GH

Bei der Redaktion eingegangen am 8. Juni 1998.

Dedicated to Professor Peter Böttcher on the Occasion of his 60th Birthday

Abstract. Metastable $CuBrSe_2$ was prepared by the fast cooling of a melt ($T \geq 400\,°C$) of copper(I) bromide and selenium in the ratio 1:2 to room temperature. The crystal structure was determined from single crystals separated from the solidified melt. The compound crystallizes isotypic to $CuXTe_2$ (X = Cl, Br, I) and $CuClSe_2$, space group $P2_1/n$ (No. 14) with $a = 7.8838(9)$ Å, $b = 4.6439(4)$ Å, $c = 11.183(1)$ Å, $\beta = 103.44(1)°$, $V = 398.2(1)$ Å^3, and $Z = 4$. The refinement converged to $R = 0.0424$ and $wR = 0.0851$ (all reflections), respectively. In the crystal structure formally neutral one-dimensional selenium chains $^1_\infty$[Se] are coordinated to copper(I) bromide. Slow cooling of the melt or heating of solid $CuBrSe_2$ to 250 °C for some hours results in the decomposition of the compound, and a mixture of $CuBrSe_3$ and CuBr is formed. DSC measurements indicate, that this decomposition starts at about 200 °C. Nevertheless, a melting point of 342 °C can be determined. In Raman spectra of $CuBrSe_2$, selenium-selenium stretching modes are found at $\nu_{Se-Se} = 241$ and 219 cm^{-1}.

Keywords: Copper halides; selenium; metastable phases; crystal structure

$CuBrSe_2$: eine metastabile Verbindung im System CuBr/Se

Inhaltsübersicht. Metastabiles $CuBrSe_2$ wurde durch schnelles Abkühlen einer Schmelze ($T \geq 400\,°C$) von Kupfer(I)-bromid und Selen im Verhältnis 1:2 auf Raumtemperatur erhalten. Die Kristallstruktur wurde an einem Einkristall bestimmt, der vom Schmelzregulus isoliert werden konnte. Die Verbindung kristallisiert isotyp zu $CuXTe_2$ (X = Cl, Br, I) und $CuClSe_2$, Raumgruppe $P2_1/n$ (Nr. 14) mit $a = 7{,}8838(9)$ Å, $b = 4{,}6439(4)$ Å, $c = 11{,}183(1)$ Å, $\beta = 103{,}44(1)°$, $V = 398{,}2(1)$ Å^3 und $Z = 4$. Die Verfeinerung konvergierte bei $R = 0{,}0424$ bzw. $wR = 0{,}0851$ (alle Reflexe). In der Kristallstruktur sind formal neutrale eindimensionale Ketten von Selenatomen $^1_\infty$[Se] an Kupfer(I)-bromid koordiniert. Kühlt man die Schmelze langsam ab oder erwärmt festes $CuBrSe_2$ für einige Stunden auf 250 °C, so zersetzt sich die Verbindung unter Bildung von $CuBrSe_3$ und CuBr. In DSC-Messungen setzt diese Zersetzung ab etwa 200 °C ein. Trotzdem kann eine Schmelztemperatur von ca. 342 °C ermittelt werden. In Ramanspektren von $CuBrSe_2$ werden Selen–Selen-Streckschwingungen bei $\nu_{Se-Se} = 241$ und 219 cm^{-1} beobachtet.

1 Introduction

The exploration of compounds formed by copper(I) halides and neutral homoatomic chalcogen molecules, that is, polymeric chains and six-membered rings, respectively, started in 1969 [1, 2]. A series of nine compounds was prepared by hydrothermal methods from the corresponding mineral acids [3]. Tellurium and the copper(I) halides form two isostructural series of compounds with the compositions CuXTe [4–6] and $CuXTe_2$ [7, 8] (X = Cl, Br, I), respectively. They all contain formally neutral infinite one-dimensional (1 D) tellurium chains $^1_\infty$[Te]. However, the compositions and crystal structures of the compounds formed by copper(I) halides and selenium depend strongly on the type of the chosen copper(I) halide. Thus $CuClSe_2$ [9] containing a screw like 1D selenium polymer $^1_\infty$[Se] is isotypic with $CuClTe_2$ contrary both to $CuBrSe_3$ [10] and $CuISe_3$ [11], which exhibit six-membered selenium rings in their crystal structures. Recently also heteroatomic neutral chalcogen chains $^1_\infty$[SeTe] and $^1_\infty$[STe] could be obtained as copper(I) halide adducts in CuXSeTe (X = Cl, Br, I) and in CuXSTe (X = Cl, Br), respectively [12, 13]. It was shown, that the chal-

* Priv.-Doz. Dr. A. Pfitzner
Prof. Dr. H. J. Deiseroth, Dipl.-Chem. T. Nilges
Anorganische Chemie
Universität-GH Siegen
D-57068 Siegen
Fax: +49 27 17 40 25 55
e-mail: pfitzner@chemie.uni-siegen.de

  0044–2313/99/625201–206 $ 17.50+.50/0

cogen chains in the corresponding compounds are relatively rigid and strongly dominate the crystal structures. Contrary the substructure formed by the copper halides is relatively flexible and fits perfectly to the different chains. The substitution of selenium in the six-membered rings in $CuXSe_3$ by tellurium provided the first examples for tellurium rich rings $Se_{6-x}Te_x$ in a solid material [14]. By these investigations it became evident that the different structures of $CuBrSe_3$ and $CuISe_3$ are due to a change in the volume ratio of the copper(I) halide and the neutral chalcogen rings. A comparison of the structural parameters of $CuClSe_2$ with those of $CuXTe_2$ makes evident that a compound with the composition $CuBrSe_2$ could also exist. However, this was not found in a phase diagram reported earlier [3]. This might be due to the preparational techniques used so far, that is, either the hydrothermal approach or the equilibrating method of stoichiometric amounts of CuBr and Se at relatively low temperatures. Here we report the synthesis and characterization of $CuBrSe_2$ obtained by fast cooling a melt of CuBr and Se in the ratio 1 : 2.

2 X-ray structure determination

A single crystal of suitable size for X-ray structure determination was separated from a fast cooled sample of $CuBrSe_2$. The crystal was fixed on top of a glass capillary and mounted on a STOE IPDS diffractometer. Experimental details are summarized in Table 1.[1)] The crystal structure was solved by direct methods and refined against F^2 using the JANA98 program package [15]. The refinement converged to a final $R = 0.0424$ using all reflections and 37 refined parameters. Table 2 contains the positional parameters, anisotropic displacement parameters are gathered in Table 3. Selected interatomic distances, angles and torsion angles are given in Table 4. For comparison the corresponding data for $CuClSe_2$ according to ref. [9] are included.

$CuBrSe_2$ is isotypic with the other copper(I) halide chalcogen adducts with the general composition $CuXQ_2$ (X = halide, Q = Se, Te) described above, see Figure 1. The most striking feature of the crystal structure are 1 D pseudo-fourfold screw-like selenium chains $^1_\infty$[Se] directing along the *b*-axis. The bond lengths *d*(Se–Se) are 2.3387(8) Å, and 2.4097(8) Å. They are only slightly larger (ca. 0.02 Å) than in $CuClSe_2$ [9], which is due to some discrepancies in the determination of the lattice constants rather than to a structural difference. If we use the lattice constants we refined from powder photographs (Guinier and diffractometer data) and the refined positions given in [9] the distances *d*(Se–Se) are equal within three σ for $CuBrSe_2$ and $CuClSe_2$. The occurrence of two significantly different bond lengths in a given chain with one about 0.04 Å smaller and the other about 0.04 Å lar-

Table 1 Crystallographic data (e.s.d.s) for the structure analysis of $CuBrSe_2$

Compound	$CuBrSe_2$
Formula weight (g mol^{-1})	301.37
Crystal size (mm^3) and colour	0.55×0.12×0.05, black
Crystal system	monoclinic
Space group	$P2_1/n$ (No. 14)
Lattice constants (Å)	$a = 7.8838(9)$
from single crystal	$b = 4.6439(4)$
	$c = 11.183(1)$
	$\beta = 103.44(1)°$
Cell volume, Z	398.2(1), 4
$\rho_{X\text{-ray}}$ (g cm^{-3})	5.025
Diffractometer	STOE IPDS, MoKα, $\lambda = 0.71073$ Å, oriented graphite monochromator
Image plate distance	70 mm
φ-range (°), $\Delta\varphi$(°)	$0 \le \varphi \le 360$, 1.0
Absorption correction	numerical, crystal description with six faces, shape optimized with X-SHAPE [21]
No. of measured images	360
Irradiation time/image (min.)	6
Temperature (°C)	25
2θ-range (°)	$3.3 < 2\theta < 52.1$
hkl-range	$-9 \le h \le 9$
	$-5 \le k \le 5$
	$-13 \le l \le 13$
No. of reflections, $R_{int.}$	5265, 0.0957
No. of independent reflections	768
No. of parameters	37
Program	JANA98 [15]
$R^{a)}(I > 3\sigma_I)$, $R^{a)}$ (all reflections)	0.0360, 0.0424
$wR^{a)}(I > 3\sigma_I)$, $wR^{a)}$ (all reflections)	0.0845, 0.0851
GooF$^{a)}$	2.78
Largest difference peak $\Delta\rho_{max}$	1.27
and hole $\Delta\rho_{min}$ (e Å^{-3})	–1.54

a) $R = \frac{\Sigma\ F_o\ \ F_c}{\Sigma\ F_o}$ $wR = \frac{\Sigma\ w\ F_o^2\ \ F_c^2\ ^2}{E\ w\ F_o^2\ ^2}$ GooF $= \frac{\Sigma\ w\ F_o^2\ \ F_c^2\ ^2}{n\ \ p}$

$w = 1/(\sigma^2(F_o^2) + (0.01\,F_o^2)^2)$

Table 2 Atomic coordinates and equivalent isotropic displacement parameters U_{eq}[a)] (in Å^2) for $CuBrSe_2$

Atom	*x*	*y*	*z*	U_{eq}
Cu	0.43001(9)	0.1367(2)	0.25185(8)	0.0264(3)
Br	0.70522(7)	0.1153(1)	0.60328(5)	0.0217(2)
Se1	0.41469(7)	0.2202(1)	0.84051(6)	0.0183(2)
Se2	0.85210(7)	–0.0050(1)	0.15534(6)	0.0172(2)

a) U_{eq} is defined as one third of the trace of the orthogonalized U^{ij} tensor.

Table 3 Anisotropic displacement parameters U^{ij} (in Å^2) for $CuBrSe_2$

Atom	U^{11}	U^{22}	U^{33}	U^{12}	U^{13}	U^{23}
Cu	0.0132(4)	0.0284(4)	0.0391(5)	0.0016(3)	0.0092(3)	0.0068(3)
Br	0.0147(3)	0.0285(3)	0.0218(3)	–0.0057(2)	0.0042(2)	0.0007(2)
Se1	0.0108(3)	0.0206(3)	0.0244(3)	–0.0016(2)	0.0059(2)	0.0004(2)
Se2	0.0115(3)	0.0177(3)	0.0244(3)	–0.0009(2)	0.0082(2)	0.0005(2)

1) Further details of the crystal structure investigations are available on request from the Fachinformationszentrum Karlsruhe, D-76344 Eggenstein-Leopoldshafen (Germany) (Fax: (+49)7247-808-666 (Mrs. S. Höhler-Schlimm); E-mail: crysdata@fiz-karlsruhe.de), on quoting the depository number CSD-410004.

Table 4 Selected interatomic distances (in Å), angles (in °), and torsion angles (in °) for $CuBrSe_2$ and for $CuClSe_2$ (data according to ref. [9], e. s. d. s are given in parentheses where available)

$CuBrSe_2$		$CuClSe_2$ [9]	
Cu–Br	2.4205(9)		
	2.436(1)		
–Se1	2.429(1)	Cu–Se1	2.409
–Se2	2.4430(9)	–Se2	2.420
Se1–Se2	2.3387(8)	Se1–Se2	2.316(4)
	2.4097(8)		2.393(3)
Se2–Br	3.3272(8)	Se2–Cl	3.193
Br–Cu–Br	108.75(3)		
Br–Cu–Se1	107.27(3)		
	113.19(4)		
Br–Cu–Se2	107.33(3)		
	114.70(4)		
Se1–Cu–Se2	105.73(3)	Se1–Cu–Se2	105.6
Se1–Se2–Se1	102.88(3)	Se1–Se2–Se1	102.9(1)
Se2–Se1–Se2	104.25(3)	Se2–Se1–Se2	104.4(1)
Se1–Se2–Se1–Se2	±43.11(3)/	Se1–Se2–Se1–Se2	±42.40/
	±61.41(3)		±62.57

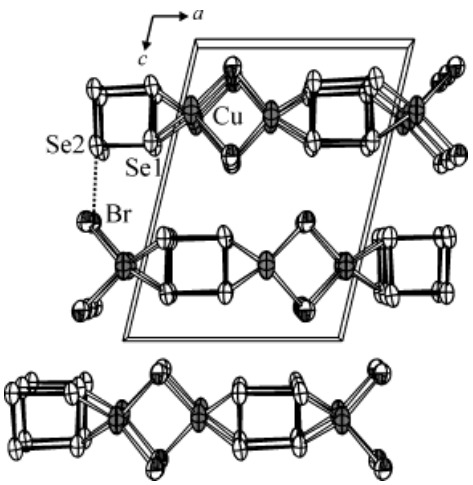

Fig. 1 Section of the crystal structure of $CuBrSe_2$. One of the short interlayer distances d(Br–Se) = 3.3272(8) Å is indicated by a dashed line. Ellipsoids represent a probability of 90%.

ger than the distance d(Se–Se) found in elemental trigonal selenium [16] is due to interactions of selenium with bromide ions from the neighboring layers (see below). This effect has already been discussed in ref. [13]. Due to the short distance d(Se2–Br) = 3.3272(8) Å the opposite bond Se2–Se1 is elongated as compared to the bond Se2–Se1 perpendicular to the Se2–Br direction. Also, some positive polarization of Se2 has to be assumed and the bond angle Se–Se–Se is somewhat smaller for Se2. Therefore this position is preferably substituted by tellurium in the case of the mixed chalcogen chains $^1_\infty$[SeTe]. The chalcogen chains are coordinated to copper on two sides and each selenium atom is bonded to one copper atom, cf. Figure 2. Only slight differences are found for the bond lengths

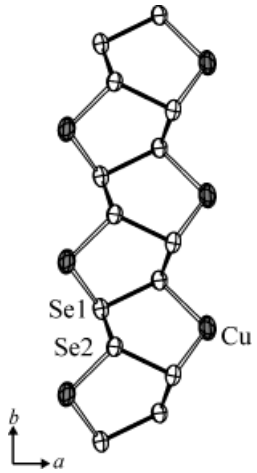

Fig. 2 $^1_\infty$[Se] chain with coordinating copper atoms. Torsion angles are Se2–Se1–Se2–Se1: ±61.4° and Se1–Se2–Se1–Se2: ±43.1°, respectively.

d(Cu–Se), both being close to $\overline{d}$ = 2.436 Å. Copper atoms are four-coordinate by two selenium atoms from one chain and to two bromide atoms. Distorted tetrahedra [$CuSe_2Br_{2/2}$] result, which are linked by the bromide ions along [0 1 0]. Due to this vertex linkage, the copper halide matrix can adapt the translational period of different chalcogen chains. The angle between the tetrahedron edges formed by the halide ions can vary in a certain range as already shown in ref. [13]. In case of $CuBrSe_2$ this angle takes a value of 72.06° which is slightly above the supposed minimum of ca. 70°. The coordination of the 1 D selenium screws by copper and the subsequent expansion of the local environment results in two-dimensional (2 D) layers with the composition $CuBrSe_2$. These layers are stacked along [0 0 1] in such a way that bromide ions form the above mentioned short interlayer contacts. Since the 3 D crystal structure is based only on these van der Waals-interactions, the graphite-like constitution of these compounds is not unexpected.

3 X-ray powder investigations

Several samples in the composition range 1 : 3 ≤ CuBr : Se ≤ 1 : 2 were equilibrated at temperatures up to 550 °C for some hours and then either fast cooled (ca. 300 °C/min) to room temperature or cooled at a rate of about 200 °C/h to room temperature. No crystalline products were obtained if the melt was quenched in ice-water. Figure 3 shows some typical X-ray powder patterns of crystalline samples obtained by the above mentioned procedure, a collection of d-spacings is given in Table 5. These measurements reveal that $CuBrSe_2$ contains a small amount of CuBr as an impurity when a stoichiometric batch is used. On the other hand $CuBrSe_2$ is the only crystalline

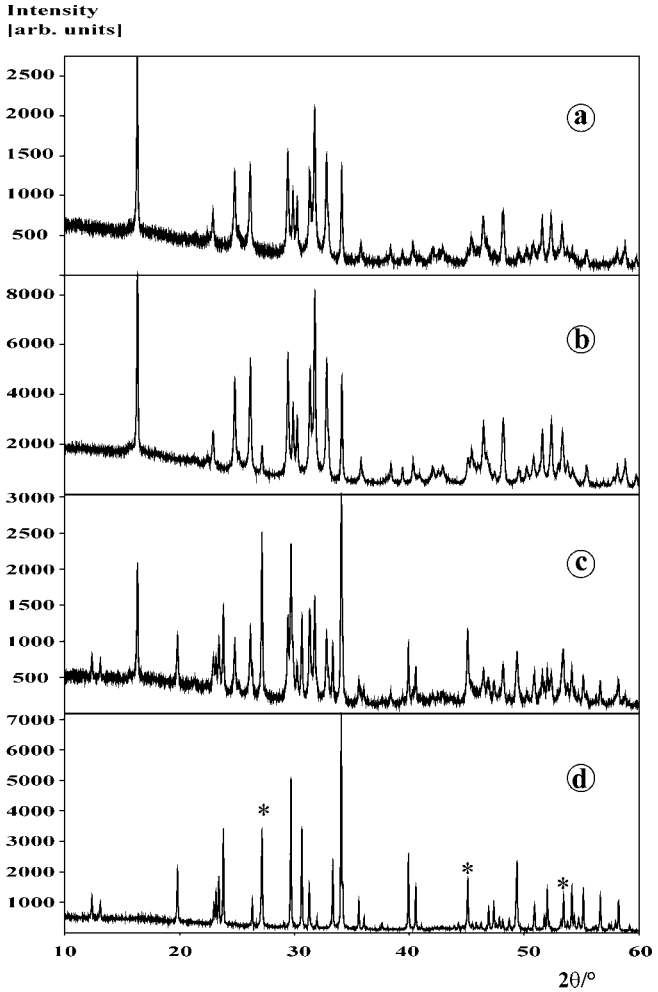

Fig. 3 X-ray powder patterns of a fast cooled melt with a nominal composition of a) $CuBr:Se = 1:3$, b) $CuBr:Se = 1:2$, c) the same sample $CuBrSe_2$ after annealing at 200 °C for 12 hours, and d) after annealing at 300 °C for three hours. The fast cooled melt contains almost pure $CuBrSe_2$. Reflections of CuBr as an impurity are marked by an asterisk (*). With increasing temperature $CuBrSe_2$ decomposes yielding $CuBrSe_3$ and CuBr as can be derived from the increasing intensities of the corresponding reflections.

phase in cases when the starting composition was $CuBr:Se = 1:3$. These samples must contain some amorphous selenium which cannot be detected by X-ray diffraction. The lattice constants of $CuBrSe_2$ extracted from these powder patterns are independent of the starting composition within a 3σ limit. The refined data are: $a = 7.886(1)$ Å, $b = 4.6442(7)$ Å, $c = 11.181(2)$ Å, $\beta = 103.44(1)°$, and $V = 398.2(2)$ Å^3. Figure 3 also shows an X-ray powder pattern of a sample with the nominal composition $CuBr:Se = 1:2$ after heating to 200 °C for 12 h and at 300 °C for 3 h, respectively. It becomes obvious that the transition of $CuBrSe_2$ to $CuBrSe_3$ is relatively fast even at this temperature. During this reaction in the solid state the selenium chains in $CuBrSe_2$ are transformed to six-membered selenium rings in $CuBrSe_3$. From high temperature X-ray photographs recorded on a Simon-Guinier camera it can be derived that the starting point and the duration for this reaction is dependent on the heating rate. The starting and the end point are 200 and 230 °C for a rate of 10 °C/h, and 230 and 255 °C for 30 °C/h, respectively. Thus the reaction takes ca. three hours at about 215 °C and only one hour at about 240 °C.

Table 5 *d*-values of $CuBrSe_2$ (reflections with $I_{obs} < 5\%$ are omitted, $CuK\alpha_1$, $\lambda = 1.54051$ Å, flat sample in transmission geometry), intensities are not listed since the pattern shows strong texture. The lattice constants determined from the powder are $a = 7.885(1)$, $b = 4.6442(7)$, $c = 11.181(2)$ Å, $\beta = 103.473(9)°$

h	*k*	*l*	d_{obs}(Å)	d_{calc}(Å)
0	0	2	5.4379	5.4367
1	1	0	3.9716	3.9725
–1	1	1	3.8862	3.8855
1	1	1	3.5935	3.5941
–1	1	2	3.4109	3.4095
1	1	2	3.0372	3.0376
–2	1	1	2.9923	2.9926
2	1	0	2.9576	2.9568
–1	1	3	2.8550	2.8545
2	0	2	2.8375	2.8375
–2	1	2	2.8185	2.8187
2	1	1	2.7322	2.7316
0	0	4	2.7181	2.7183
–3	0	1	2.6288	2.6285
–2	0	4	2.5100	2.5107
0	1	4	2.3457	2.3460
–3	1	2	2.2371	2.2377
1	2	1	2.1494	2.1491
–1	2	2	2.1082	2.1076
–1	1	5	2.0116	2.0126
–2	2	1	1.9963	1.9970
2	2	0	1.9864	1.9863
0	2	3	1.9556	1.9552
–2	2	2	1.9435	1.9427
–3	1	4	1.9333	1.9328
3	0	3	1.8921	1.8917
–3	0	5	1.8872	1.8876

4 Raman spectra

Figure 4 shows a Raman spectrum recorded for $CuBrSe_2$. The spectrum is dominated by two intense bands at $\nu = 241$ cm^{-1} and at $\nu = 219$ cm^{-1}, respectively. These modes are assigned to stretching modes of the $^1_\infty$[Se] polymer (from comparison with the other isotypic $CuXQ_2$ compounds [17]) and show a stronger splitting than the corresponding modes of trigonal selenium (237 cm^{-1}, 234 cm^{-1} [18]). The stronger splitting of the Se–Se vibrational modes, as compared to trigonal selenium, are either due to a stronger coupling in $CuBrSe_2$ or to the different bond lengths *d*(Se–Se) mentioned above. In addition a weak band is observed at 264 cm^{-1} (assigned to ν_{Cu-Se} [19]) and some further bands below 150 cm^{-1}. The latter are due to either selenium lattice vibrations or to Cu–Br stretching modes.

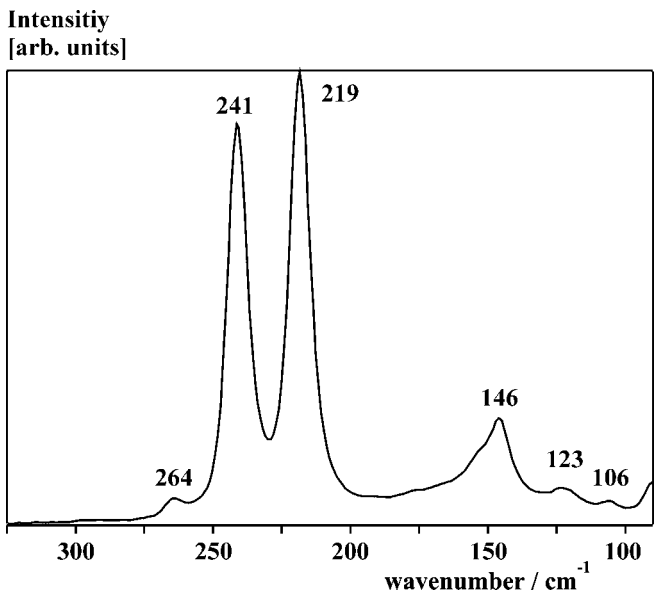

Fig. 4 Raman spectrum of metastable $CuBrSe_2$, recorded with an excitation wavelength of 1064 nm. The strong bands at 241 and 219 cm^{-1}, respectively, are assigned to Se–Se stretching modes.

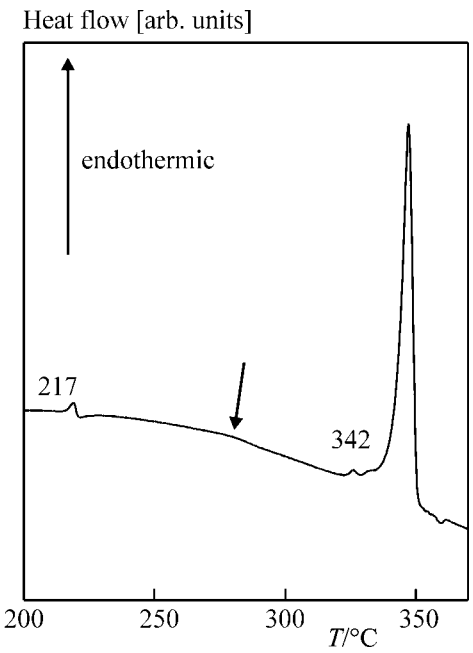

Fig. 5 DSC curve of $CuBrSe_2$ (RT → 400 °C, 10 °C min^{-1}). Numbers given in the diagram are onset temperatures (217 °C: mp. (Se), 342 °C: mp. ($CuBrSe_2$)). The arrow indicates the change in the slope of the baseline, which is related to the start of the decomposition of $CuBrSe_2$. Under these conditions, i. e. a cooling rate of 10 °C min^{-1}, no $CuBrSe_2$ is formed when cooling down from the melt. From subsequent heating curves the formation of $CuBrSe_3$ can be derived.

5 Thermal analyses

Samples of $CuBrSe_2$, obtained by the fast cooling method, were characterized by means of DTA and DSC measurements at different heating rates. Figure 5 shows a typical DSC curve. It exhibits a small endothermic effect at about 217 °C, which is due to some (amorphous) selenium impurities and a stronger endothermic effect at 342 °C, which is the melting/decomposition point of $CuBrSe_2$. Due to the relatively high heating rate of 5 °C/min (as compared to the rate of 10 or 30 °C/h in the X-ray experiments) the transformation of $CuBrSe_2$ to $^2/_3\,CuBrSe_3 + {}^1/_3\,CuBr$ cannot be detected by an exothermic effect in the DSC measurements as one might expect. The only indication for the beginning transformation is a very slight (exothermic) anomaly of the base line at about 270 °C. The temperature of this reproducible tiny effect depends on the heating rate and is probably due to the starting decomposition of $CuBrSe_2$. The cooling curve and subsequent heating curves show a different characteristic insofar as an additional strong endothermic effect at 336 °C occurs. This temperature is in good accord with the peritectic decomposition temperature of $CuBrSe_3$ (T = 338 °C) reported in [3].

6 Discussion

The hitherto unknown adduct of copper(I) bromide to 1 D selenium chains $CuBrSe_2$ was characterized by single crystal X-ray diffraction. It is isotypic to the other copper(I) halide adducts to chalcogen chains with a nominal composition $CuXQ_2$ (X = halide, Q = chalcogen). It is the first compound of this series which shows a transition in the solid state. During this transition the composition changes from $CuBrSe_2$ to $CuBrSe_3$, and the $^1_\infty$[Se] polymers are rearranged to six-membered rings Se_6.

These investigations show that the synthesis of metastable materials does not necessarily benefit from low temperature techniques [20]. The existence of $CuBrSe_2$ and the method of its preparation give some evidence, that the selenium chains in the molten mixture with copper bromide are already coordinated by copper. Obviously the arrangement found in the solid compound is locally maintained in the melt. It is possible to transform this melt to a metastable crystalline material if an appropriate cooling rate is applied. If the cooling rate is too small no $CuBrSe_2$ can be detected, if it is too fast only amorphous products are obtained. Preliminary experiments with mixtures of CuCl and Se show the same results insofar as $CuClSe_2$ is readily formed. Contrary to $CuBrSe_2$ this compound is thermodynamically stable and no transformation to $CuClSe_3$ (which is not yet known) is observed. Further investigations of the copper(I) halide-selenium melts are necessary to check these assumptions carefully. The copper(I) chalcogen halides seem to be appropriate compounds for studies of transition rates in the solid state.

7 Experimental

$CuBrSe_2$ was obtained by reacting stoichiometric amounts of copper(I) bromide (> 99%, Riedel de Haën) and selenium (99.999%, ChemPur) in evacuated quartz ampoules. CuBr was purified by recrystallization from aqueous HBr prior to use. The reaction mixture was heated to 550 °C and kept at that temperature for 6 hours. Then the ampoule was removed from the oven and cooled to room temperature within 5 minutes. $CuBrSe_2$ was obtained as black, needle shaped crystals. Upon grinding the color turned to dark-red. For comparison also batches with a composition different from Cu Br : Se = 1 : 2 were treated by this method. In each case more or less pure $CuBrSe_2$ was obtained. If the ampoules were cooled much slower to room temperature only a mixture of $CuBrSe_2$ and $CuBrSe_3$ or even solely $CuBrSe_3$ was observed.

Single crystal X-ray data were collected on an IPDS (STOE), see above. Powder diffraction data were recorded on a D5000 (SIEMENS) at room temperature, and on a Guinier-Simon camera (NONIUS) at high temperature, using monochromatized Cu Kα_1 radiation (λ = 1.54051 Å) and silicon as an external standard. Raman spectra were recorded on a RFS100/S (BRUKER) in a backscattering mode using a Nd : YAG laser with an excitation wavelength of 1064 nm. Thermal analyses were performed with a DTA L62 (LINSEIS), and a DSC7 (PERKIN ELMER). Transition temperatures were determined from onset values.

Acknowledgment. The authors thank *Prof. Lutz* for the possibility to use the Raman spectrometer. This work has been financially supported by the Deutsche Forschungsgemeinschaft and the Fonds der Chemischen Industrie.

References

[1] A. Rabenau, H. Rau, G. Rosenstein, *Naturwissenschaften* **1969**, *56*, 137.
[2] A. Rabenau, H. Rau, *Solid State Comm.* **1969**, *7*, 1281.
[3] A. Rabenau, H. Rau, G. Rosenstein, *Z. Anorg. Allg. Chem.* **1970**, *374*, 43.
[4] W. Milius, *Z. Anorg. Allg. Chem.* **1990**, *586*, 175.
[5] P. M. Carkner, H. M. Haendler, *J. Solid State Chem.* **1976**, *18*, 183.
[6] J. Fenner, A. Rabenau, *Z. Anorg. Allg. Chem.* **1976**, *426*, 7.
[7] J. Fenner, *Acta Crystallogr. B* **1976**, *32*, 3084.
[8] W. Milius, *Z. Naturforsch. B* **1989**, *44*, 990.
[9] W. Milius, A. Rabenau, *Z. Naturforsch. B* **1988**, *43*, 243.
[10] H. M. Haendler, P. M. Carkner, S. M. Boudreau, R. A. Boudreau, *J. Solid State Chem.* **1979**, *29*, 35.
[11] W. Milius, A. Rabenau, *Mater. Res. Bull.* **1987**, *22*, 1493.
[12] A. Pfitzner, S. Zimmerer, *Z. Anorg. Allg. Chem.* **1995**, *620*, 969.
[13] A. Pfitzner, S. Zimmerer, *Z. Anorg. Allg. Chem.* **1996**, *621*, 853.
[14] A. Pfitzner, S. Zimmerer, *Z. Kristallogr.* **1997**, *212*, 203.
[15] V. Petricek, JANA98, Institute of Physics, Academy of Sciences of the Czech Republic, Prague, Czech Republic **1998**.
[16] P. Cherin, P. Unger, *Inorg. Chem.* **1967**, *6*, 1589.
[17] A. Pfitzner, T. Nilges, to be published.
[18] K. Nagata, K. Ishibashi, Y. Miyamoto, *Japan. J. Appl. Phys.* **1981**, *20*, 463.
[19] J. D. Sarfati, G. R. Burns, *Spectrochim. Acta A* **1994**, *50*, 2125.
[20] A. Stein, S. W. Keller, T. E. Mallouk, *Science* **1993**, *259*, 1558.
[21] X-SHAPE, STOE, Darmstadt **1996**.